February 5, 1998 @ 13:00

FINAL
IN-43-CR
OCIT

Land Cover Analysis of Temperate Asia Final Report

Department of Geography
University of Maryland, College Park

Summary: Satellite data from the advanced very high resolution radiometer (AVHRR) instrument were used to produce a general land cover distribution of temperate Asia (referred to hence as Central Asia) from 1982, starting with the NOAA-7 satellite, and continuing through 1991, ending with the NOAA-11 satellite. Emphasis was placed upon delineating the arid and semi-arid zones of Central Asia (largely Mongolia and adjacent areas), mapping broad categories of aggregated land cover, and upon studying photosynthetic capacity increases in Central Asia from 1982 to 1991.

Early on in our study in became apparent that the photosynthetic activity of terrestrial vegetation in temperate Asia increased from 1981 to 1991, seemingly accompanied by a possible increase in the length of the growing season. The regions of greatest increase lie between 45 ^{o} N and 70^{o} N in the center of the area we proposed to study. This is also the portion of Central Asia where marked warming has been reported in the spring time (Chapman and Walsh, 1993) and where the early disappearance of snow cover has also been reported (Groisman et al., 1994). Our AVHRR satellite data showed a higher northern latitude increase in the amplitude of the seasonal cycle of photosynthetic capacity similar to recently reported increases in atmospheric CO_2 seasonal amplitudes (Keeling et al., 1996). Thus both satellite and atmospheric CO_2 data indicate increased higher northern latitude biosphere activity and suggest the global carbon cycle has responded to interannual fluctuations in temperature which, although small at the global scale, are regionally highly significant. It was mandatory to evaluate these possible changes in increased higher northern latitude biosphere activity to determine in which ecological zones they were occurring.

NOAA AVHRR Satellite Data

The National Oceanic and Atmospheric Administration's (NOAA) series of sun-synchronous polar-orbiting meteorological satellites orbit at an altitude of ~850 km and have a daytime overpass time of ~ 1430 hours local solar time immediately after launch (Price, 1991). The advanced very high resolution radiometer (AVHRR) sensor scans ~55^{o} from nadir and complete coverage of the earth is available twice daily with a spatial resolution of ~5.5 x 3.3 km at the satellite subpoint. Daily data from channels 1 (0.55-0.70 μm), 2 (0.73-1.1 μm), and 5 (11.5-12.5 μm) were used with a scan angle of 40^{o} or less (45 pixel delete from each end of every scan line), processed to produce a normalized difference vegetation index (NDVI) of (2-1)/(2+1), and formed into bimonthly maximum value composites after Holben (1986). Channel 5 was used as a cloud filter where every pixel cooler than ~0^{o} C was labeled as a cloud. Holben (1986) and Holben and Fraser (1984) have shown that maximum value vegetation index composites simultaneously minimize scan angle, atmospheric effects, clouds, and all other degrading effects upon the vegetation index. Every global location has ≥10 potential daytime data values to choose from every ~15-day period. Global area coverage (GAC) data, with a nadir spatial resolution of ~ 4-km, were used in this study.

Confusion sometimes results when vegetation indices are used to describe research results because all vegetation indices are sensor-dependent. It is thus instructive to review how vegetation index data correlate to more commonly-measured vegetation or meteorological variables, such as biomass production or precipitation.

The normalized difference vegetation index is a non-destructive estimate of the photosynthetic potential or capacity of the area measured (Sellers 1985 and 1987). Consequently, when normalized difference vegetation index measurements are made over time, they provide information on the history of the photosynthetic potential or capacity. This has been shown to be highly related to total biomass production in grassland systems. This assumption has been tested in the Sahelian zone of West Africa where Tucker et al. (1985) and Prince (1991) have shown multi-temporal NOAA AVHRR normalized difference vegetation index data to be directly related to herbaceous above-ground biomass production.

Biomass production and green vegetation density are usually closely related to precipitation in grasslands and savannas. Precipitation ceases to be the primary factor in primary production when the rainfall is greater than ~700-800 mm/yr (Lamotte and Bourliere, 1983; Le Houerou and Hoste, 1977). The relationship of precipitation to green vegetation density and biomass, or primary production, depends upon the amount and timing of the rainfall, evapotranspiration and runoff, soil infiltration, and the ability of vegetation to respond to rainfall, among other factors.

Consequently, there is a strong and direct relationship between precipitation and the normalized difference vegetation index in most grassland systems, although other factors such as temperature, type of precipitation, timing, intensity, etc. are also important (Lauenroth, 1979; Malo and Nicholson, 1990; Nicholson et al., 1990; Rutherford, 1980; Seely, 1978).

Processing of Images:

Bi-monthly maximum-value composite images (day 1 to day 15, and from day 16 to the end of every month, to ensure correspondence with months) were obtained from 1-April to 1-November of every year from 1982 to 1992. Each bimonthly composite image was visually checked for registration errors using large lakes. Any composite images with mis-registration were reformed by mapping each day's data separately and registering all days of data within the respective composite to common coastline reference points using World Data Base II. Resulting registration errors were thus minimized and in all but a few unusual cases were less than ±2 picture elements or ~±12 km. Mean and standard deviation images were then formed from the bimonthly normalized difference vegetation index composite images from each year. Each year's mean normalized difference vegetation image was adjusted to 1986 using the respective calibration adjustment for that year (Price, 1987; Holben et al., 1990; Brest and Rossow, 1992; Kaufman and Holben, 1993; and Los, 1993).

Compensation for atmospheric effects is important when NOAA AVHRR data are used anywhere (Tanre et al., 1992); this is especially true when spectral vegetation indices are used from arid and semi-arid areas. The modest green vegetation signal from these areas is potentially greatly compromised by atmospheric effects.

The principal sources of atmospheric effects in AVHRR channel 1 and channel 2 data are from differential molecular scattering, aerosol scattering, ozone absorption, and water vapor absorption, often complicated by viewing geometry and illumination. These effects are highly variable, and at times are compensating (Tanre et al., 1992). While we have not applied any atmospheric correction the data, we have used the normalized difference vegetation index maximum-value composites formed for each bimonthly period tend to minimize atmospheric effects (Holben, 1986).

Results

The NDVI data set for middle Asia covers the area from the Caspian Sea to Manchuria (figure 1). Figure 1 indicates a good correspondence to actual land cover, where the arid belt extends from the Taklamakan Desert of East Turkistan in a northeast direction into Mongolia. Within Mongolia, a zonation is apparent resembling the desert zone (< 100 mm/yr precipitation), desert steppe (~100-200 mm/yr), the steppe zone (~200-300 mm/yr), the forest-steppe zone (>300 mm/yr), and the taiga zone. Figure 1 is a qualitative representation of land cover, since specific comparisons to ground data have not yet been performed, but are in progress.

Table 1. Simplified ecological aggregation of land cover classes for Mongolia as determined in this study.

Ecological Region	**Area (km^2)**	**% of Total Area**
Forest or Taiga Zone	415,136	26.5%
Mixed Forest and Steppe Zone	108,139	6.9%
Mountain Steppe Zone	169,101	10.8%
Steppe Zone	251,940	16.1%
Desert Steppe Zone	389,700	24.9%
Desert	230,101	14.7%
Total Mongolian Area:	1,564,117	100.0%

The satellite data in figure 1 indicate two different climatic gradients in the Mongolia/Inner Mongolia region and adjacent areas. Within Mongolia, moving from the forest and forest steppe zones near Ulaanbaatar (44 ^{o}N, 102 ^{o}E) in a southwestern direction into the Gobi

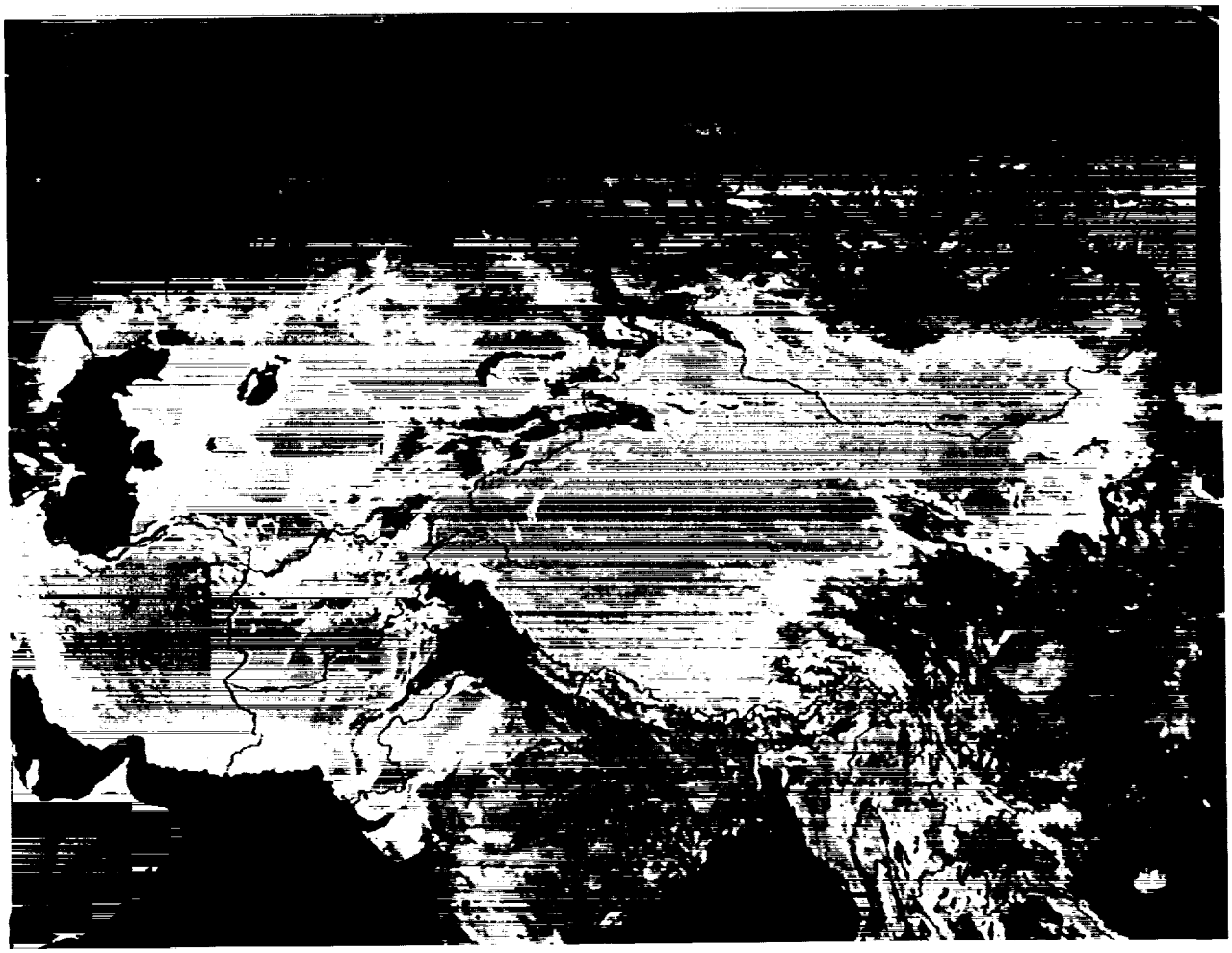

Figure 1. The average normalized difference vegetation index image from 1982-1991, formed from daily global area coverage NOAA AVHRR data processed into bi-monthly maximum value composite images from 1-April to 1-October. The spatial resolution is ~6 km for every grid cell location in an equal area mapping projection. This figure for all of Central or Middle Asian data shows a good correspondence to broad zonations of land cover. See also Table 1 for an areal summary of this figure as it pertains to Mongolia.

Desert, one moves first into the steppe zone, then the desert-steppe zone, and finally into the Gobi Desert proper. Selecting representative locations for the forest/forest-steppe zone at 44 ^{o} N, 102 ^{o} E, for the steppe zone at 45.7 ^{o} N by 103.7 ^{o} E, at 47.3 ^{o} N by 105.3 ^{o} E for the desert steppe zone, and at 49 ^{o} N by 107 ^{o} E for the Gobi Desert proper and plotting monthly average normalized difference vegetation indices from 1982 to 1992, the general qualitative nature of climatic and primary production gradients from these regions is evident over this broad roughly north east-to-south west gradient (figure 2a).

At the same time, moving from Inner Mongolia at 122 ^{o} E to the west along the 44^{o} N latitude parallel, the average normalized difference vegetation indices increase at a local maxima at ~ 117 ^{o} E and then begin to decrease with progressive movement to the west along the 44 ^{o} N parallel. The minima along this parallel is reached in the Gobi Desert at 44 ^{o} N by 97 ^{o} E (figure 2b). These variations in the normalized difference vegetation index are in general agreement with climatic and primary production gradients.

Work is presently underway to compare precipitation data from specific locations in Mongolia and Inner Mongolia to coincident NDVI data, and to compare grassland total biomass production data from specific locations to the NDVI data. Furthermore, AVHRR 1-km data have been obtained, will be processed, and compared to the same ground data for the 1990-1997 period for which the satellite data exist. It is assumed that 1-km data will be required for many location-specific studies, since the spatial complexity can be substantial in the desert desert-steppe, and steppe zones. We intend to pursue similar investigations to Tucker et al. (1991) and Prince (1991) to describe land cover variation and primary production features of the grasslands of the Mongolian steppes, through cooperation with scientists working in these areas.

Photosynthetic Increases in Central Asia

Changes in the Asian summer maxima normalized difference vegetation index at northerly latitudes are plotted in Fig. 3, as characterized by changes in the July and August average NDVI. At northern latitudes this broad measure of the seasonal maximum approximates the seasonal amplitude because winter-time NDVI there is close to zero. The seasonal maximum NDVI, by this definition, increased by 8% to 14%, depending on the latitude, from 1981 through 1990 (Fig. 3). Because NDVI is a measure of photosynthetic capacity of vegetation (Asrar et al., 1984; Myneni et al.,1995), this increase indicates that the photosynthetic activity of plants at higher northern latitudes >45^{o} N increased by 10% during the 1980s. A similar but slightly larger increase (14%) is indicated

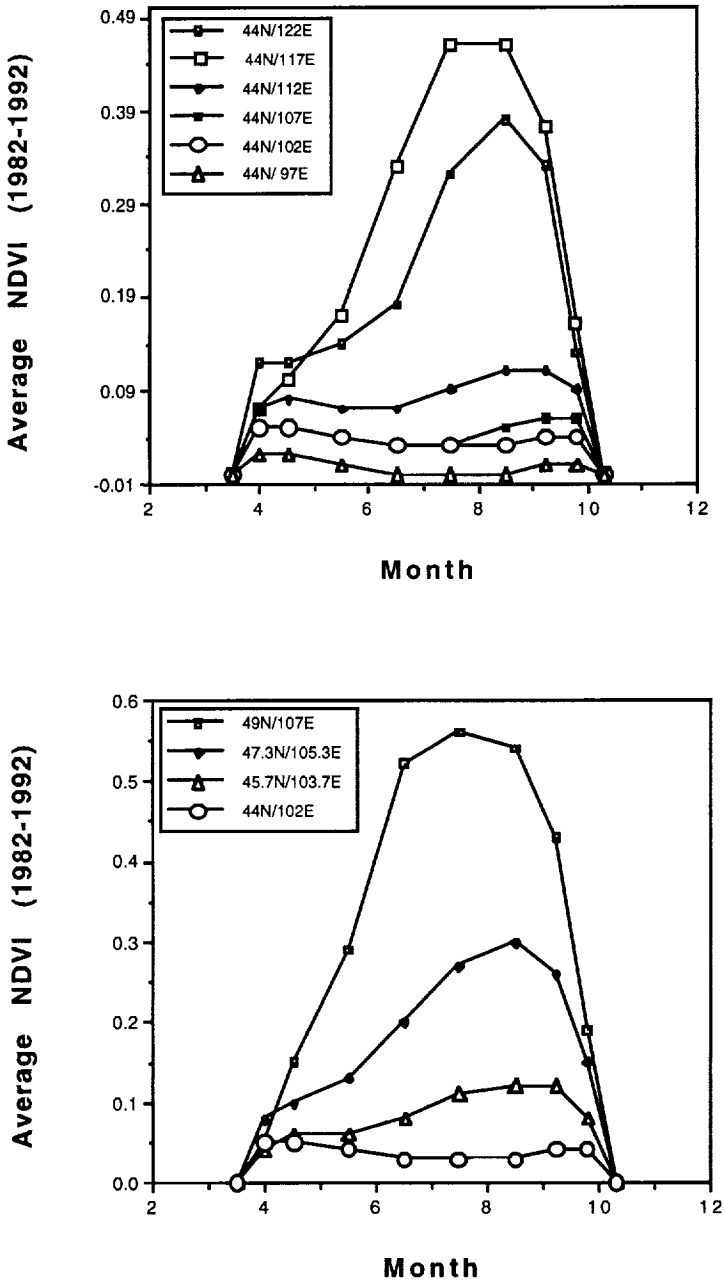

Figure 2. Normalized difference vegetation time variations by month, averaged from 1982-1992, at selected locations in Mongolia and adjacent areas. Each datum represents a spatial average of ~400 km^2. (Bottom) represents moving from the forest and forest-steppe zone of Mongolia into the Gobi Desert as noted for the 4 selected locations along this roughly north to south gradient. (Top) represents a corresponding gradient moving along the 44th parallel, from Inner Mongolia into the Gobi Desert of Mongolia. Refer also to figure 1 and Table 1.

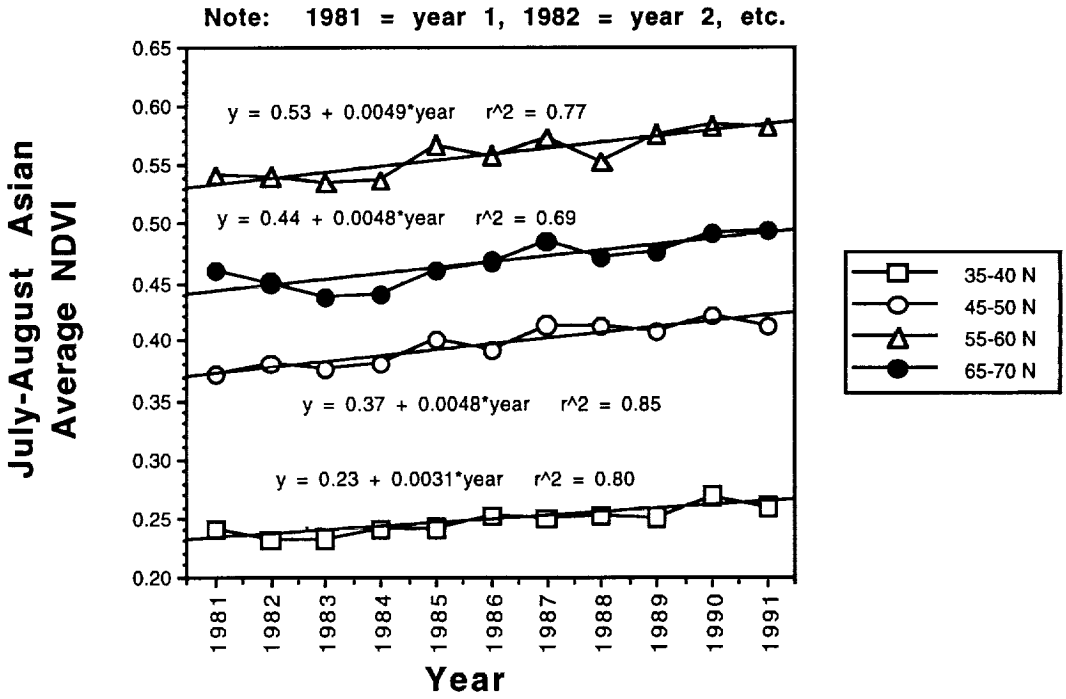

Figure 3. Asian zonal average normalized difference vegetation index values from 45-70o N for July-August and May-September of 1982 to 1991. Note the increasing trend with time as reported in Myneni et al. (1997).

by changes in the seasonal cycle of atmospheric CO_2 measured at Point Barrow, Alaska for the same time period (Keeling et al, 1996). A recent study has also reported increased biomass deposition in Central Asia from tree-ring analysis in Mongolia (Jacoby et al, 1996).

In Central Asia, a band of increasing NDVI across Asia to the western Pacific ocean was evident. In this band, a broad region near Lake Baikal in Siberia adjacent to Mongolia is most affected. Outside this band, northern China and northeastern Siberia were also strongly affected.

In general, the regions of greatest increase in NDVI are remote from the oceans and are north of 50° N. The prominent bands of increased NDVI referred to above in both Central Asia correspond generally with areas of high NDVI (Fig. 1). Thus, most of the areas where changes in NDVI amplitude and seasonality were observed are also regions of significant vegetation density. Notable exceptions are

several arctic regions in the far north of Asia where NDVI rose sharply from low initial values.

References

Asrar, G., Fuchs, M., Kanemasu, E. T. and Hatfield, J. L. 1984. Estimating absorbed photosynthetic radiation and leaf area index from spectral reflectance in wheat. *Agron. J.* **76**, 300-306.

Brest, C.L. and Rossow, W.B., 1992. Radiometric calibration and monitoring of NOAA AVHRR data for ISCCP. *Int. J. Remote Sens.*, **13**, 235-273.

Chapman, W. L. and Walsh, J. E., 1993. Recent variations of sea ice and air temperatures in high latitudes. *Bull. Am. Met. Soc* **74**, 33-47.

Groisman, P. Ya., Karl, T. R. and Knight, T. W. , 1994. Observed impact of snow cover on the heat balance and the rise of continental spring temperatures. *Science* **263**, 198-200.

Holben, B.N., 1986, Characteristics of maximum-value composite images from temporal AVHRR data. *International Journal of Remote Sensing*, **7**, 1417-1434.

Holben, B.N. and Fraser, R.S., 1984, Red and near-infrared sensor response to off-nadir viewing. *International Journal of Remote Sensing,* **5,** 145-160.

Holben, B. N., Kaufman, Y. J., and Kendall, J., 1990, NOAA-11 AVHRR visible and near-infrared inflight calibration. *Int. J. Remote Sens.* **11**, 1511-1519.

Jacoby, G. C., D'Arrigo, R. D. and Davaajamts, T. , 1996. Mongolian tree rings and 20th-century warming. *Science* **273**, 771-773.

Kaufman, Y. . and Holben, B. N., 1993. Calibration of the AVHRR visible and near- bands by atmospheric scattering, ocean glint, and desert reflection. *Int. J. Remote Sens.,* **14,** 21-52.

Keeling, C. D., Chin, J. F. S. and Whorf, T. P., 1996. Increased activity of northern vegetation inferred from atmospheric CO2 measurements. *Nature* **382**, 146-149.

Lamotte, M. and Bourliere, F., 1983, Energy flow and nutrient cycling in tropical savannas. In *Tropical Savannas, Ecosystems of the World,* **13,** F. Bourliere, editor (Elsevier, New York), pp. 583-606.

Lauenroth, W.K., 1979, Grassland primary production: North American grasslands in perspective. In *Perspectives in Grassland Ecology*, edited by N. French, Springer-Verlag, New York, pp. 3-24.

Le Houerou, H.N. and Hoste, C.H., 1977, Rangeland production and annual rainfall relations in the Mediterranean Basin and in the African Sahelo-Sudanian Zone. *J. Range Manage.,* **30,** 181-189.

Los, S.O., 1993, Calibration adjustment of the NOAA AVHRR normalized difference vegetation index without recourse to component channel 1 and 2 data. *Int. J. Remote Sens.*, **14**, 1907-1917.

Malo, A.R, and Nicholson, S.N.,1990, A study of rainfall and vegetation dynamics in the African Sahel using normalized difference vegetation index. *J. Arid Environ.*, **19**, 1-24..

Myneni, R. B., Hall, F. G., Sellers, P. J., and Marshak, A. L., 1995. The interpretation of spectral vegetation indices. *IEEE Trans. Geosci. Remote Sens.* **33**, 481-486

Myneni, R. B., Keeling, C.D., Tucker, C. J., Asrar, G., and Nemani, R., 1997. Increased plant growth in the northern high latitudes from 1981 to 1991. *Nature*, **386**, 698-702.

Nicholson, S.E., Davenport, M.L., and Malo, A.R., 1990, A comparison of the vegetation response to rainfall in the Sahel and East Africa, using normalized difference vegetation index from NOAA AVHRR. *Climate Change,* **17**, 209-242.

Price, J., 1987, Calibration of satellite radiometers and the comparison of vegetation indices. *Remote Sens. Environ.*, **21**, 15-27.

Price, J., 1991, Timing of the NOAA afternoon passes. *Int. J. Remote Sens.*, **12**, 193-198.

Prince, S.D. 1991, Satellite remote sensing of primary production: comparison of results for Sahelian grasslands 1981-1988. *Int. J. Remote Sens.*, **12**,1301-1312.

Rutherford, M.C., 1980, Annual plant production-precipitation relations in arid and semi-arid regions. *So. African J. Science,* **76,** 53-56.

Sellers, P.J., 1985, Canopy reflectance, photosynthesis, and transpiration. *Int. J. Remote Sens.*, **6,** 1335-1372.

Sellers, P.J., 1987, Canopy reflectance, photosynthesis, and transpiration. II. The role of biophysics in the linearity of their interdependence *Remote Sens. Environ.*, **21,** 143-183.

Seely, M.K., 1978, Grassland productivity: The desert end of the curve. *So. Afr. J. Sci.*, **74,** 295-297.

Tanre, D., Holben, B. N., and Kaufman, Y. J., 1992. Atmospheric correction algorithm for NOAA-AVHRR products: theory and application. *IEEE Trans. Geosci. Remote Sens.*, **30**, 231-248.

Tucker, C.J., C.L. Vanpraet, M.J. Sharman, and G. Van Ittersum, 1985, Satellite remote sensing of total herbaceous biomass production in the Senegalese Sahel: 1980-1984. *Remote Sens. Environ.*, **17,** 233-249.

Tucker, C.J., Dregne, H.E., and Newcomb, W.W., 1991, Expansion and contraction of the Sahara Desert from 1980 to 1990. *Science*, **253**, 299-301.

Tucker, C. J., Newcomb, W. W., and H. E. Dregne, 1994. AVHRR data sets for the determination of desert spatial extent. *Int. J. Remote Sens.* **15**, 3547-3566.